



1

Iodine chemistry after dark

2 Alfonso Saiz-Lopez¹, John M.C. Plane², Carlos A. Cuevas¹, Anoop S. Mahajan³, Jean-François

3 Lamarque⁴ and Douglas E. Kinnison⁴

4 ¹Department of Atmospheric Chemistry and Climate, Institute of Physical Chemistry
5 Rocasolano, CSIC, Madrid, Spain

6

7 ²School of Chemistry, University of Leeds, Leeds, UK

8

9 ³Indian Institute of Tropical Meteorology, Pune, India

10

11 ⁴Atmospheric Chemistry Observations and Modelling, NCAR, Colorado, USA

12 Correspondence to: A. Saiz-Lopez (a.saiz@csic.es)



1 **Abstract**

2 Little attention has so far been paid to the nighttime atmospheric chemistry of iodine species.
3 Current atmospheric models predict a buildup of HOI and I₂ during the night that leads to a spike
4 of IO at sunrise, which is not observed by measurements. In this work, electronic structure
5 calculations are used to survey possible reactions that HOI and I₂ could undergo at night in the
6 lower troposphere, and hence reduce their nighttime accumulation. The new reaction NO₃ + HOI
7 → IO + HNO₃ is proposed, with a rate coefficient calculated from statistical rate theory over the
8 temperature range 260 - 300 K and at a pressure of 1000 hPa to be $k(T) = 2.7 \times 10^{-12} (300 \text{ K} / T$
9 $)^{2.66} \text{ cm}^3 \text{ molecule}^{-1} \text{ s}^{-1}$. This reaction is included in two atmospheric models, along with the
10 known reaction between I₂ and NO₃, to explore a new nocturnal iodine radical activation
11 mechanism. The results show that this iodine scheme leads to a considerable reduction of
12 nighttime HOI and I₂, which results in the enhancement of more than 25% of nighttime ocean
13 emissions of HOI + I₂ and the removal of the anomalous spike of IO at sunrise. We suggest that
14 active nighttime iodine can also have a considerable, so far unrecognized, impact on the
15 reduction of the NO₃ radical levels in the MBL and hence upon the nocturnal oxidizing capacity
16 of the marine atmosphere. The effect of this is exemplified by the indirect effect on dimethyl
17 sulfide (DMS) oxidation.

18

19

20

21



1 **1. Introduction**

2 Active nighttime iodine chemistry was first evidenced a decade ago when it was shown that
3 nocturnal I₂ emitted by macroalgae could react with NO₃ leading to the formation of IO and
4 OIO, which were measured in the coastal marine boundary layer (MBL) at Mace Head, Ireland
5 (Saiz-Lopez and Plane, 2004). The nitrate radical has also been recently suggested as a nocturnal
6 loss of CH₂I₂, which helps to reconcile observed and modelled concentrations of this iodocarbon
7 over the remote MBL (Carpenter et al., 2015). However, most of the work on reactive
8 atmospheric iodine has focused on the use of daytime observations and models to assess its role
9 in the catalytic destruction of ozone and the oxidizing capacity of the troposphere (e.g. Saiz-
10 Lopez et al. (2012b) and references therein). In the MBL, iodine, along with bromine, catalysed
11 ozone destruction contributes up to 45% of the observed daytime depletion (Read et al., 2008;
12 Mahajan et al., 2010a), although this contribution shows large geographical variability (Mahajan
13 et al., 2012; Gómez Martín et al., 2013; Prados-Roman et al., 2015b; Volkamer et al., 2015).
14 Iodine compounds have also been implicated in the formation of aerosols, although the
15 mechanisms and magnitudes of these processes are not fully understood (O'Dowd et al., 2002;
16 McFiggans et al., 2004; Saunders and Plane, 2005; Pechtl et al., 2006; Saiz-Lopez et al., 2006;
17 Mahajan et al., 2009a; Hoffmann et al., 2001; Gomez Martin et al., 2013; Sommariva et al.,
18 2012; Allan et al., 2015; Roscoe et al., 2015). Reactive forms of inorganic iodine may also
19 contribute to the oxidation of elemental mercury over the tropical oceans (Wang et al., 2014). In
20 recent years, iodine sources and chemistry have also been implemented in global models
21 demonstrating the effect of iodine chemistry in the oxidation capacity of the global marine
22 troposphere (Ordóñez et al., 2012; Saiz-Lopez et al., 2012a; Saiz-Lopez et al., 2014; Sherwen et
23 al., 2016).



1 Iodine is emitted into the atmosphere from the ocean surface in both organic and inorganic
2 forms. The main organic compounds emitted are methyl iodide (CH_3I), ethyl iodide ($\text{C}_2\text{H}_5\text{I}$), and
3 propyl iodide (1- and 2- $\text{C}_3\text{H}_7\text{I}$), chloriodomethane (CH_2ICl), bromiodomethane (CH_2IBr), and
4 diiodomethane (CH_2I_2) (Carpenter, 2003; Butler et al., 2007; Jones et al., 2010; Mahajan et al.,
5 2012). However, these organic compounds contribute only up to a third of the MBL iodine
6 loading (Großmann et al., 2013; Mahajan et al., 2010a; Jones et al., 2010; Prados-Roman et al.,
7 2015b). Inorganic emissions of HOI and I_2 , which result from the deposition of O_3 at the ocean
8 surface and subsequent reaction with I^- ions in the surface microlayer, account for the main
9 source of iodine in the MBL (Carpenter et al., 2013). Recent laboratory experiments have shown
10 that HOI is the major compound emitted, and provided parameterizations of the fluxes of both
11 species depending on wind speed, temperature, and the concentrations of O_3 and I^- (Carpenter et
12 al., 2013; MacDonald et al., 2014). These parameterized fluxes of HOI and I_2 have then been
13 used in a one-dimensional model to study the diurnal evolution of the IO and I_2 mixing ratios at
14 the Cape Verde Atmospheric Observatory (CVAO) (Carpenter et al., 2013; Lawler et al., 2014).
15 The model simulations replicate well the levels and general diurnal profiles of IO and I_2 ,
16 although an early morning ‘dawn spike’ in IO is predicted by the models, but has not been
17 observed (Read et al., 2008; Mahajan et al., 2010a). The morning peak predicted by current
18 iodine chemistry models is due to a buildup of the emitted I_2 and HOI (which is converted into
19 $\text{I}_2/\text{IBr}/\text{ICl}$ through heterogeneous sea-salt recycling) over the course of the night, followed by
20 rapid photolysis at sunrise.

21 Traditionally it has been thought that iodine chemistry has a negligible effect on oxidizing
22 capacity of the nocturnal marine atmosphere. As a consequence, unlike the demonstrated effect
23 of iodine on the levels of daytime oxidants, the impact of active iodine upon the main nighttime



1 oxidant, NO_3 , remains an open question. This is important given that in many parts of the ocean
2 the $\text{NO}_3 + \text{DMS}$ reaction is at least as important as $\text{OH} + \text{DMS}$ in oxidizing DMS (Allan et al.,
3 2000), and hence a reduction of NO_3 may have an effect in the production of SO_2 and methane
4 sulfonic acid (MSA). Here, we discuss possible mechanisms of nighttime iodine radical
5 activation and their potential effect on nighttime iodine ocean fluxes and the currently modeled
6 dawn spike in IO. A new reaction of HOI with NO_3 is proposed, supported by theoretical
7 calculations. We explore the implications of this new reaction both for iodine and NO_3
8 chemistries.

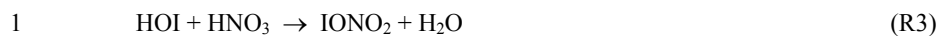
9

10 **2. Nocturnal iodine radical activation mechanism**

11 We use the reaction mechanism that has recently been described in a global modelling study by
12 Saiz-Lopez et al. (2014). In addition to the reactions included in that scheme, we also include
13 nighttime gas-phase reactions based on the theoretical calculations described below. The
14 additional reactions are listed in Table 1 and a scheme with this new nocturnal chemistry is
15 included in Figure 1.

16 To the best of our knowledge, reactions of HOI specific to night time have not been studied,
17 either theoretically or through laboratory experiments. Currently, HOI is thought to build up
18 overnight until sunrise, with only heterogeneous uptake on seasalt aerosol as a nighttime loss
19 process (Saiz-Lopez et al., 2012b; Simpson et al., 2015). In addition to the well known $\text{I}_2 + \text{NO}_3$
20 reaction (R1) (Chambers et al., 1992), here we consider several possible HOI reactions that could
21 occur at night, in the absence of photolysis and OH:





3

4 **3. Theoretical calculations**

5 In order to explore the feasibility of reactions 2–4 taking place under the conditions of the lower
6 troposphere, we carried out electronic structure calculations using the hybrid density
7 functional/Hartree-Fock B3LYP method from within the Gaussian 09 suite of programs (Frisch
8 et al., 2009), combined with a G2 level basis set for I (Glukhovtsev et al., 1995) and the standard
9 6-311+g(2d,p) triple zeta basis set for O, N and H. Following geometry optimizations of the
10 relevant points on the potential energy surfaces, and the determination of their corresponding
11 vibrational frequencies and (harmonic) zero-point energies, energies relative to the reactants
12 were obtained. Spin-orbit splittings of -17 and -5 kJ mol^{-1} were applied to the energies I and IO,
13 respectively; these were estimated by comparing the theoretical and experimental bond energies
14 of I_2 and IO (Plane et al., 2006; Kaltsoyannis and Plane, 2008).

15 Reaction 2 is endothermic by 9 kJ mol^{-1} and so, within the expected error of $\pm 10 \text{ kJ mol}^{-1}$ at this
16 level of theory, might be reasonably fast. However, the transition state of the reaction, which is
17 illustrated in Figure 2(a), is 73 kJ mol^{-1} above the reactants and so this reaction will not occur at
18 tropospheric temperatures. Reaction 3 is exothermic by 11 kJ mol^{-1} . An HOI--HNO₃ complex
19 first forms (Figure 2(b)), which is 21 kJ mol^{-1} below the reactants. However, this complex
20 rearranges to the $\text{IONO}_2 + \text{H}_2\text{O}$ products via the cyclic transition state shown in Figure 2(c),
21 which is 110 kJ mol^{-1} above the reactants.



1 The stationary points on the potential energy surface (PES) for reaction 4 are illustrated in Figure
2 3. HOI and NO₃ associate to form a complex which is 24 kJ mol⁻¹ below the reactant entrance
3 channel. H-atom transfer involves a submerged transition state to form a IO--HNO₃ complex,
4 which can then dissociate to the products IO + HNO₃. Overall, the reaction is exothermic by 11
5 kJ mol⁻¹. The vibrational frequencies, rotational energies and geometries (in Cartesian
6 co-ordinates) of these intermediates are listed in Table 2.

7 The rate coefficient for reaction 4 was then estimated using Rice-Ramsperger-Kassel-Markus
8 (RRKM) theory, employing a multi-well energy-grained master equation solver based on the
9 inverse Laplace transform method - MESMER (Master Equation Solver for Multi-well Energy
10 Reactions) (Roberston et al., 2014). The reaction proceeds via the formation of the excited
11 HOI--NO₃ complex from HOI + NO₃. This complex can then dissociate back to the reactants or
12 rearrange to the IO--HNO₃ intermediate complex over the transition state, which can in turn
13 dissociate to the products IO + HNO₃. Either of intermediates can also be stabilized by collision
14 with the third body (N₂). The time evolution of all these possible outcomes is modelled using the
15 master equation.

16 The internal energies of the intermediates on the PES were divided into a contiguous set of
17 grains (width 10 cm⁻¹), each containing a bundle of rovibrational states calculated with the
18 molecular parameters in Table 2. Each grain was then assigned a set of microcanonical rate
19 coefficients linking it to other intermediates, calculated by RRKM theory. For dissociation to
20 products or reactants, microcanonical rate coefficients were determined using inverse Laplace
21 transformation to link them directly to the capture rate coefficient, k_{capture} . For reaction 4 and the
22 reverse reaction IO + HNO₃ involving neutral species, k_{capture} was set to a typical capture rate
23 coefficient of $2.5 \times 10^{-10} (T/300 \text{ K})^{1/6} \text{ cm}^3 \text{ molecule}^{-1} \text{ s}^{-1}$, where the small positive temperature



1 dependence is characteristic of a long-range potential governed by dispersion and dipole-dipole
2 forces (Georgievskii and Klippenstein, 2005).

3 The probability of collisional transfer between grains was estimated using the exponential down
4 model, where the average energy for downward transitions was set to $\langle \Delta E \rangle_{\text{down}} = 300 \text{ cm}^{-1}$ for
5 N_2 as the third body (Gilbert and Smith, 1990). MESMER determines the temperature- and
6 pressure-dependent rate coefficient from the full microcanonical description of the system time
7 evolution by performing an eigenvector/eigenvalue analysis (Bartis and Widom, 1974). The
8 resulting rate coefficient over the temperature range 260 - 300 K at a pressure of 1000 hPa is
9 $k_4(T) = 2.7 \times 10^{-12} (300 \text{ K} / T)^{2.66} \text{ cm}^3 \text{ molecule}^{-1} \text{ s}^{-1}$. Because the intermediate complexes are
10 not strongly bound, and the transition state and products are below the entrance channel, the only
11 products formed in reaction 4 under atmospheric conditions are $\text{IO} + \text{HNO}_3$. The absence of a
12 barrier above the entrance channel means that the uncertainty in k_4 principally arises from the
13 estimated capture rate coefficient and so is likely to be no more than a factor of 2.

14 Note that NO_3 also reacts with CH_2I_2 with a rate constant $\sim 2\text{-}4 \times 10^{-13} \text{ cm}^3 \text{ molecule}^{-1} \text{ s}^{-1}$, which
15 can have a significant effect on nighttime CH_2I_2 concentration (Carpenter et al., 2015). However
16 the products of this reaction are still uncertain (Nakano et al., 2006; Carpenter et al., 2015) and
17 its rate is considerably slower than that of R4.

18 In summary, the only likely gas-phase reactions that I_2 and HOI undergo in the nighttime
19 troposphere are R1 and R4, respectively. These are included in the model reaction scheme to
20 examine their impacts on the evolution of iodine species in the atmosphere.

21

22



1 **4. Atmospheric modelling**

2 We use two atmospheric chemical transport models to study *i*) the impact of this new chemistry
3 on the nighttime chemistry and partitioning of iodine species, and *ii*) the resulting geographical
4 distribution of nocturnal iodine and impact on NO₃ within the global marine boundary layer.

5 The first model, Tropospheric HALogen chemistry MOdel (THAMO), is used for a detailed
6 kinetics study of the impact of the different reactions shown in Table 1 as well as to assess which
7 uptake rates best reproduce observations from a field study at the CVAO (Carpenter et al., 2011).
8 THAMO has been used in the past to study iodine chemistry at the CVAO and further details
9 including the full chemical scheme can be found elsewhere (Saiz-Lopez et al., 2008; Mahajan et
10 al., 2009b; Mahajan et al., 2010b; Mahajan et al., 2010a; Lawler et al., 2014; Read et al., 2008).
11 Briefly, THAMO is a 1-D chemistry transport model with 200 stacked boxes at a vertical
12 resolution of 5m (total height 1 km). The model treats iodine, bromine, O₃, NO_x and HO_x
13 chemistry, and is constrained with typical measured values of other chemical species in the
14 MBL: [CO]=110 nmol mol⁻¹; [DMS]=30 pmol/mol; [CH₄]=1820 nmol mol⁻¹; [ethane]=925
15 pmol/mol; [CH₃CHO]=970 pmol/mol; [HCHO]=500 pmol/mol; [isoprene]=10 pmol/mol;
16 [propane]=60 pmol/mol; [propene]=20 pmol/mol. The average background aerosol surface area
17 (ASA) used is 1x10⁻⁶ cm² cm⁻³ (Read et al., 2008; Read et al., 2009; Lee et al., 2009; Lee et al.,
18 2010). The model is initialized at midnight and the evolution of iodine species, O₃, NO_x and HO_x
19 is followed until the model reaches steady state.

20 The second model is the global 3D chemistry-climate model CAM-Chem (Community
21 Atmospheric Model with chemistry, version 4.0), which is used to study the impact of reactions
22 1 and 4 on a global scale. The model includes a comprehensive chemistry scheme to simulate the



1 evolution of trace gases and aerosols in the troposphere and the stratosphere (Lamarque et al.,
2 2012). The model runs with the iodine and bromine chemistry schemes from previous studies
3 (Fernandez et al., 2014; Saiz-Lopez et al., 2014; Saiz-Lopez et al., 2015), including the
4 photochemical breakdown of bromo- and iodo-carbons emitted from the oceans (Ordóñez et al.,
5 2012) and abiotic oceanic sources of HOI and I₂ (Prados-Roman et al., 2015a). CAM-Chem has
6 been configured in this work with a horizontal resolution of 1.9° latitude by 2.5° longitude and 26
7 vertical levels, from the surface to ~40km altitude. All model runs in this study were performed
8 in the specified dynamics mode (Lamarque et al., 2012) using offline meteorological fields
9 instead of an online calculation, to allow direct comparisons between different simulations. This
10 offline meteorology consists of a high frequency meteorological input from a previous free
11 running climatic simulation.

12

13 **5. Results and discussion**

14 Of the possible nocturnal iodine activation reactions involving the inorganic iodine source gases
15 I₂ and HOI, only reactions R1 and R4 appear to be likely candidates (see Section 3). We
16 therefore designed two modelling scenarios: Scenario 1 (S1), without nighttime reactions of I₂ or
17 HOI with NO₃; and Scenario 2 (S2), including reactions R1 and R4 for the degradation of HOI
18 and I₂ by NO₃. In the one-dimensional model THAMO, the I₂ and HOI are injected into the
19 atmosphere from the ocean surface using the flux parameterizations derived from laboratory
20 experiments (MacDonald et al., 2014; Carpenter et al., 2013). Figure 4 shows the resulting
21 diurnal evolution of the HOI and I₂ mixing ratios in the two scenarios. The I₂ mixing ratio peaks
22 during the night in both the scenarios due to quick loss by photolysis during the daytime. By



1 contrast, HOI peaks during the daytime due to its production through the reaction of IO with
2 HO₂. In the first scenario, without the inclusion of reactions R1 and R4, Figure 4 (right-hand side
3 panels) shows that HOI and I₂ both build up during the night, reaching a concentration peak just
4 before dawn. This is especially noticeable for I₂ as the daytime concentrations are much lower
5 than during the night. For both species, inclusion of reactions with NO₃ causes a decrease in their
6 respective nocturnal concentrations (Fig. 4, left-hand side panels). The inclusion of reactions R1
7 and R4 also leads to a modelled I₂ concentration which is in better agreement with the
8 observations of the molecule made at CVAO (Lawler et al., 2014), reaching peak values of
9 about 1 pmol/mol, as compared to about 3 pmol/mol for the scenario without nighttime reactions.
10 An additional consequence of including reactions R1 and R4 is the significant increase of the
11 sea-air fluxes of HOI and I₂ at night due to their atmospheric removal by NO₃ (Fig. 4, bottom
12 panel).

13 It should be noted that during nighttime the uptake of emitted species such as I₂ and HOI, and the
14 uptake of reservoir species such as IONO₂, can play a major role in the cycling of iodine.
15 Observations at CVAO show that I₂ peaked at about 1 pmol/mol during the night and that ICl
16 was not detected above the 1 pmol/mol detection limit of the instrument (Lawler et al., 2014). In
17 order to match these observations, we need to reduce the uptake and heterogeneous recycling of
18 iodine species. The uptake rates of chemical species on the background seasalt aerosols are
19 determined by their uptake coefficients (γ). The database of mass accommodation and/or uptake
20 coefficients is rather sparse and essentially limited to I₂, HI, HOI, ICI, IBr on pure water/ice and
21 on sulphuric acid particles (Sander et al., 2006). Other iodine species which are likely to undergo
22 uptake onto aerosol are OIO, HIO₃, INO₂, IONO₂, I₂O₂ (Saiz-Lopez et al., 2012a; Sommariva et
23 al., 2012). Uptake of HOI is very uncertain, with $\gamma(\text{HOI})$ ranging from 2×10^{-3} to 0.3 depending



1 on the surface composition and state (Holmes et al., 2001). Sommariva et al. (2012) assumed
2 $\gamma(\text{HOI})$ to be 0.6, similar to the value for HOBr measured by Wachsmuth et al. (2002). In the
3 case of IONO₂, the uptake coefficient has not been measured, with most models using values of
4 0.1 (von Glasow et al., 2002; Saiz-Lopez et al., 2008; Mahajan et al., 2009b; Mahajan et al.,
5 2010b; Mahajan et al., 2010a; Leigh et al., 2010; Sommariva et al., 2012; Lawler et al., 2014).
6 The modelled levels of I₂ and ICl change with different values of uptake coefficients. To match
7 the CVAO I₂ and ICl observations (Lawler et al., 2014), we have used $\gamma = 0.01$ for HOI and
8 IONO₂, which is within the uncertainty in the literature, and assumed that 80% is recycled as I₂.
9 Further measurements of these dihalogen species are needed to better constrain their
10 heterogeneous recycling on seasalt aerosols.

11 Figure 5 shows the diurnal evolution of IO, NO₃ and IONO₂ in both model scenarios. Although
12 the daytime peak values of IO are well reproduced in both scenarios, reaching about 1.5
13 pmol/mol around noon similar to the ground-based observations (Read et al., 2008), the inclusion
14 of reactions R1 and R4 leads to the removal of the dawn spike in IO, which is predicted by
15 current iodine models but was not observed at CVAO (Read et al., 2008; Mahajan et al., 2010a).
16 The IO dawn spike predicted by models is due to a buildup of the emitted I₂ and HOI (which is
17 converted into I₂/IBr/ICl through heterogeneous recycling) over the night, followed by rapid
18 photolysis after first sunlight. However, due to the considerable removal of HOI and I₂ through
19 the night due to reaction with ambient NO₃, this spike does not appear in the second scenario,
20 leading to a modification of the diurnal profile of IO that better matches with observations.

21 Reactions R1 and R4 also reduce the NO₃ mixing ratio (Fig. 4, middle panels). In scenario 1, the
22 NO₃ is modelled to peak at about 14 pmol/mol just before dawn. However, the inclusion of
23 reactions R1 and R4 leads to near complete depletion of NO₃ close to the surface, with the peak



1 level at the surface reaching only 2 pmol/mol, since reactions R1 and R4 become the main
2 atmospheric loss processes for NO_3 in the lower MBL. These reactions lead however to the
3 buildup of IONO_2 during the night (Fig. 5, bottom panels). In the absence of reactions R1 and
4 R4, significant levels of IONO_2 are seen only at dawn and dusk since no other reactions produce
5 IONO_2 at night, and during the day IONO_2 is removed by photolysis. However, with continuous
6 conversion of I_2 and HOI to IONO_2 by reactions R1 and R4 in scenario 2, IONO_2 is modelled to
7 reach up to 3 pmol/mol in the nocturnal MBL.

8 Given the associated uncertainty in the theoretical estimate of the k_4 , we used THAMO to assess
9 the sensitivity of surface NO_3 to k_4 . Figure 6 shows that NO_3 is in fact highly coupled to k_4 , with
10 the expected uncertainty in k_4 of a factor of 2 (see above) giving rise to a similar uncertainty in
11 NO_3 . A laboratory measurement of k_4 should therefore be undertaken in the future.

12 We now implement the nighttime reactions in the 3D global model (CAM-Chem) to assess the
13 resulting geographical distributions and impacts of these reactions. We have also run two
14 different scenarios in CAM-Chem, the first without R1 and R4 in the chemical scheme, and the
15 second including the new nighttime iodine chemistry. Figure 7 shows how the inclusion of R1
16 and R4 reduces globally the nighttime concentrations of I_2 and HOI . The plots correspond to the
17 midnight averaged (from 00LT to 01LT) differences between the model scenarios. Considerable
18 reductions of up to 0.5 and 10 pmol/mol (i.e. up to 100% removal) are observed for I_2 and HOI ,
19 respectively, particularly over coastal polluted regions where continental pollution outflow leads
20 to higher levels of NO_3 in the nighttime MBL. Major shipping routes also show strong nocturnal
21 iodine activity due to the characteristically high NO_x , and resulting NO_3 , associated with
22 shipping emissions.



1 Figure 8 shows the effect of this nocturnal chemistry on the concentrations of IONO₂ and NO₃.
2 As in the previous figure, the plots correspond to the nighttime averaged difference between the
3 second and the first scenarios. The maps show an increase of IONO₂ of up to 15 pmol/mol
4 (~600%) over polluted coastal areas, due to efficient conversion of NO₃ into IONO₂. The bottom
5 panel of Figure 7 shows the expected decrease of NO₃ levels associated with the inclusion of
6 reactions R1 and R4, with decreases of up to ~4 pmol/mol (up to 60%) over marine polluted
7 regions. We model global percentage reductions in the NO₃ concentrations of 7.1% (60S-60N),
8 with nitrate removal of up to 80% in non-polluted remote oceanic regions with low NO₃ levels.
9 This in turn can affect the modelled oxidation of DMS by NO₃. We estimate that the reduction in
10 NO₃, due to the inclusion of R1 and R4, results in a model increase in DMS levels of up to 7
11 pmol/mol (about 20%) in marine regions affected by continental pollution outflow (Fig. 9). We
12 therefore suggest that the inclusion of the new nighttime iodine chemistry can have a large, so far
13 unrecognized, impact on the nocturnal oxidizing capacity of the marine atmosphere.

14 The hourly evolution of the main species involved in this study is shown in Figures 10 and 11,
15 which include the levels of HOI, I₂, IONO₂ and NO₃ in the MBL over regions where nocturnal
16 iodine is modelled to be particularly active. The first region is located within the Mediterranean
17 Sea, an area that shows large differences during the summer months when high ozone levels
18 drive large emissions of HOI and I₂ from the sea, and the high levels of NO₃ at nighttime make
19 this chemistry especially important. The hourly average in August is shown in Figure 10 for
20 HOI, IONO₂ and I₂. HOI and IONO₂ (Fig 10) are the species whose concentration differ most
21 between scenarios as HOI is removed and IONO₂ produced by R4 (and, to a lesser extent, R1).
22 Over the coastal region of the Baja California Peninsula, the modelled differences between the



1 two scenarios are even higher than over the Mediterranean Sea (Figure 11). Large differences in
2 MBL NO_3 , up to 28%, are modelled during the night.

3

4 **6. Summary and conclusions**

5 The viability of the reaction of HOI with NO_2 , HNO_3 and NO_3 has been studied by theoretical
6 calculations. The results indicate that only the reaction of HOI with NO_3 , to yield $\text{IO} + \text{HNO}_3$, is
7 possible under tropospheric conditions. The inclusion of this reaction, along with that of $\text{I}_2 +$
8 NO_3 , has a number of significant implications: *i*) nocturnal iodine radical chemistry is activated;
9 *ii*) this causes enhanced nighttime oceanic emissions of HOI and I_2 ; *iii*) nighttime iodine species
10 are partitioned into high levels of IONO_2 ; *iv*) the IO spike, modelled by current iodine models
11 but not shown by observations, is removed; and, *v*) a reduction of the levels of nitrate radical in
12 the MBL, with the associated less efficient oxidation of DMS, which has important implications
13 for our understanding of the nocturnal oxidizing capacity of the marine atmosphere.

14

15 **Acknowledgments**

16 This work was supported by the Spanish National Research Council (CSIC). The National
17 Center for Atmospheric Research (NCAR) is funded by the National Science Foundation NSF.
18 The Climate Simulation Laboratory at NCAR's Computational and Information Systems
19 Laboratory (CISL) provided the computing resources (ark:/85065/d7wd3xhc). As part of the
20 CESM project, CAM-Chem is supported by the NSF and the Office of Science (BER) of the US
21 Department of Energy. This work was also sponsored by the NASA Atmospheric Composition



1 Modeling and Analysis Program Activities (ACMAP, number NNX11AH90G).

2

3 **References**

4 Allan, B. J., McFiggans, G., Plane, J. M. C., Coe, H., and McFadyen, G. G.: The nitrate radical
5 in the remote marine boundary layer, *Journal of Geophysical Research: Atmospheres*, 105,
6 24191-24204, 10.1029/2000jd900314, 2000.

7 Allan, J. D., Williams, P. I., Najera, J., Whitehead, J. D., Flynn, M. J., Taylor, J. W., Liu, D.,
8 Darbyshire, E., Carpenter, L. J., Chance, R., Andrews, S. J., Hackenberg, S. C., and McFiggans,
9 G.: Iodine observed in new particle formation events in the Arctic atmosphere during
10 ACCACIA, *Atmos. Chem. Phys.*, 15, 5599-5609, 10.5194/acp-15-5599-2015, 2015.

11 Bartis, J. T., and Widom, B.: Stochastic models of the interconversion of three or more chemical
12 species, *J. Chem. Phys.*, 60, 3474-3482, doi: 10.1063/1.1681562, 1974.

13 Butler, J. H., King, D. B., Lobert, J. M., Montzka, S. A., Yvon-Lewis, S. A., Hall, B. D.,
14 Warwick, N. J., Mondeel, D. J., Aydin, M., and Elkins, J. W.: Oceanic distributions and
15 emissions of short-lived halocarbons, *Global Biogeochem. Cycles*, 21, GB1023,
16 10.1029/2006gb002732, 2007.

17 Carpenter, L. J.: Iodine In the marine Boundary Layer, *Chem. Rev.*, 103 (12), 4953-4962, 2003.

18 Carpenter, L. J., Fleming, Z. L., Read, K. A., Lee, J. D., Moller, S. J., Hopkins, J. R., Purvis, R.
19 M., Lewis, A. C., Müller, K., Heinold, B., Herrmann, H., Fomba, K. W., Pinxteren, D., Müller,
20 C., Tegen, I., Wiedensohler, A., Müller, T., Niedermeier, N., Achterberg, E. P., Patey, M. D.,



- 1 Kozlova, E. A., Heimann, M., Heard, D. E., Plane, J. M. C., Mahajan, A., Oetjen, H., Ingham, T.,
2 Stone, D., Whalley, L. K., Evans, M. J., Pilling, M. J., Leigh, R. J., Monks, P. S., Karunaharan,
3 A., Vaughan, S., Arnold, S. R., Tschirter, J., Pöhler, D., Frieß, U., Holla, R., Mendes, L. M.,
4 Lopez, H., Faria, B., Manning, A. J., and Wallace, D. W. R.: Seasonal characteristics of tropical
5 marine boundary layer air measured at the Cape Verde Atmospheric Observatory, *J. Atmos.*
6 *Chem.*, 67, 87-140, 10.1007/s10874-011-9206-1, 2011.
- 7 Carpenter, L. J., MacDonald, S. M., Shaw, M. D., Kumar, R., Saunders, R. W., Parthipan, R.,
8 Wilson, J., and Plane, J. M. C.: Atmospheric iodine levels influenced by sea surface emissions of
9 inorganic iodine, *Nature Geosci*, 6, 108-111, 10.1038/ngeo1687, 2013.
- 10 Carpenter, L. J., Andrews, S. J., Lidster, R. T., Saiz-Lopez, A., Fernandez-Sanchez, M., Bloss,
11 W. J., Ouyang, B., and Jones, R. L.: A nocturnal atmospheric loss of
12 CH_2I_2 in the remote marine boundary layer, *J. Atmos. Chem.*,
13 10.1007/s10874-015-9320-6, 2015.
- 14 Fernandez, R. P., Salawitch, R. J., Kinnison, D. E., Lamarque, J. F., and Saiz-Lopez, A.:
15 Bromine partitioning in the tropical tropopause layer: implications for stratospheric injection,
16 *Atmos. Chem. Phys.*, 14, 13391-13410, 10.5194/acp-14-13391-2014, 2014.
- 17 Frisch, M., Trucks, G., Schlegel, H., Scuseria, G., Robb, M., Cheeseman, J., Scalmani, G.,
18 Barone, V., Mennucci, B., and Petersson, G.: Gaussian 09, Revision A. 1. Wallingford, CT:
19 Gaussian, Inc, 2009.
- 20 Georgievskii, Y., and Klippenstein, S. J.: Long-range transition state theory, *J. Chem. Phys.*, 122,
21 194103, doi: 10.1063/1.1899603, 2005.



- 1 Gilbert, R. G., and Smith, S. C.: Theory of Unimolecular and Recombination Reactions,
2 Blackwell, Oxford, 1990.
- 3 Glukhovtsev, M. N., Pross, A., McGrath, M. P., and Radom, L.: Extension of Gaussian-2 (G2)
4 theory to bromine- and iodine-containing molecules: Use of effective core potentials, J. Chem.
5 Phys., 103, 1878-1885, 1995.
- 6 Gomez Martin, J. C., Galvez, O., Baeza-Romero, M. T., Ingham, T., Plane, J. M. C., and Blitz,
7 M. A.: On the mechanism of iodine oxide particle formation, Phys. Chem. Chem. Phys., 15,
8 15612-15622, 10.1039/c3cp51217g, 2013.
- 9 Gómez Martín, J. C., Mahajan, A. S., Hay, T. D., Prados-Román, C., Ordóñez, C., MacDonald,
10 S. M., Plane, J. M. C., Sorribas, M., Gil, M., Paredes Mora, J. F., Agama Reyes, M. V., Oram, D.
11 E., Leedham, E., and Saiz-Lopez, A.: Iodine chemistry in the eastern Pacific marine boundary
12 layer, Journal of Geophysical Research: Atmospheres, 118, 887-904, 10.1002/jgrd.50132, 2013.
- 13 Großmann, K., Frieß, U., Peters, E., Wittrock, F., Lampel, J., Yilmaz, S., Tschritter, J.,
14 Sommariva, R., von Glasow, R., Quack, B., Krüger, K., Pfeilsticker, K., and Platt, U.: Iodine
15 monoxide in the Western Pacific marine boundary layer, Atmos. Chem. Phys., 13, 3363-3378,
16 10.5194/acp-13-3363-2013, 2013.
- 17 Hoffmann, T., O'Dowd, C. D., and Seinfeld, J. H.: Iodine oxide homogeneous nucleation: An
18 explanation for coastal new particle production, Geophys. Res. Lett., 28, 1949-1952, 2001.



- 1 Holmes, N. S., Adams, J. W., and Crowley, J. N.: Uptake and reaction of HOI and IONO₂ on
2 frozen and dry NaCl/NaBr surfaces and H₂SO₄, Phys. Chem. Chem. Phys., 3, 1679-1687,
3 10.1039/b100247n, 2001.
- 4 Jones, C. E., Hornsby, K. E., Sommariva, R., Dunk, R. M., von Glasow, R., McFiggans, G., and
5 Carpenter, L. J.: Quantifying the contribution of marine organic gases to atmospheric iodine,
6 Geophys. Res. Lett., 37, L18804, 2010.
- 7 Kaltsoyannis, N., and Plane, J. M. C.: Quantum chemical calculations on a selection of iodine-
8 containing species (IO, OIO, INO₃, (IO)₂, I₂O₃, I₂O₄ and I₂O₅) of importance in the atmosphere.,
9 Phys. Chem. Chem. Phys., 10, 1723-1733, 2008.
- 10 Lamarque, J. F., Emmons, L. K., Hess, P. G., Kinnison, D. E., Tilmes, S., Vitt, F., Heald, C. L.,
11 Holland, E. A., Lauritzen, P. H., Neu, J., Orlando, J. J., Rasch, P. J., and Tyndall, G. K.: CAM-
12 chem: description and evaluation of interactive atmospheric chemistry in the Community Earth
13 System Model, Geosci. Model Dev., 5, 369-411, 10.5194/gmd-5-369-2012, 2012.
- 14 Lawler, M. J., Mahajan, A. S., Saiz-Lopez, A., and Saltzman, E. S.: Observations of I₂ at a
15 remote marine site, Atmos. Chem. Phys., 14, 2669-2678, 10.5194/acp-14-2669-2014, 2014.
- 16 Lee, J. D., Moller, S. J., Read, K. A., Lewis, A. C., Mendes, L., and Carpenter, L. J.: Year-round
17 measurements of nitrogen oxides and ozone in the tropical North Atlantic marine boundary layer,
18 Journal of Geophysical Research: Atmospheres, 114, n/a-n/a, 10.1029/2009jd011878, 2009.
- 19 Lee, J. D., McFiggans, G., Allan, J. D., Baker, A. R., Ball, S. M., Benton, A. K., Carpenter, L. J.,
20 Commane, R., Finley, B. D., Evans, M., Fuentes, E., Furneaux, K., Goddard, A., Good, N.,



- 1 Hamilton, J. F., Heard, D. E., Herrmann, H., Hollingsworth, A., Hopkins, J. R., Ingham, T.,
2 Irwin, M., Jones, C. E., Jones, R. L., Keene, W. C., Lawler, M. J., Lehmann, S., Lewis, A. C.,
3 Long, M. S., Mahajan, A., Methven, J., Moller, S. J., Müller, K., Müller, T., Niedermeier, N.,
4 O'Doherty, S., Oetjen, H., Plane, J. M. C., Pszenny, A. A. P., Read, K. A., Saiz-Lopez, A.,
5 Saltzman, E. S., Sander, R., von Glasow, R., Whalley, L., Wiedensohler, A., and Young, D.:
6 Reactive Halogens in the Marine Boundary Layer (RHAMBLe): the tropical North Atlantic
7 experiments, *Atmos. Chem. Phys.*, 10, 1031-1055, 10.5194/acp-10-1031-2010, 2010.
- 8 Leigh, R. J., Ball, S. M., Whitehead, J., Leblanc, C., Shillings, A. J. L., Mahajan, A. S., Oetjen,
9 H., Dorsey, J. R., Gallagher, M., Jones, R. L., Plane, J. M. C., Potin, P., and McFiggans, G.:
10 Measurements and modelling of molecular iodine emissions, transport and photodestruction in
11 the coastal region around Roscoff, *Atmos. Chem. Phys.*, 10, 11823-11838, 2010.
- 12 MacDonald, S. M., Gómez Martín, J. C., Chance, R., Warriner, S., Saiz-Lopez, A., Carpenter, L.
13 J., and Plane, J. M. C.: A laboratory characterisation of inorganic iodine emissions from the sea
14 surface: dependence on oceanic variables and parameterisation for global modelling, *Atmos.*
15 *Chem. Phys.*, 14, 5841-5852, 10.5194/acp-14-5841-2014, 2014.
- 16 Mahajan, A., Oetjen, H., Lee, J. D., Saiz-Lopez, A., McFiggans, G., and Plane, J. M. C.: High
17 bromine oxide concentrations in the semi-polluted boundary layer, *Atmos. Environ.*, 43, 3811-
18 3818, 2009a.
- 19 Mahajan, A. S., Oetjen, H., Saiz-Lopez, A., Lee, J. D., McFiggans, G. B., and Plane, J. M. C.:
20 Reactive iodine species in a semi-polluted environment, *Geophys. Res. Lett.*, 36, L16803,
21 doi:16810.11029/12009GL038018, 2009b.



- 1 Mahajan, A. S., Plane, J. M. C., Oetjen, H., Mendes, L., Saunders, R. W., Saiz-Lopez, A., Jones,
2 C. E., Carpenter, L. J., and McFiggans, G. B.: Measurement and modelling of tropospheric
3 reactive halogen species over the tropical Atlantic Ocean, *Atmos. Chem. Phys.*, 10, 4611-4624,
4 2010a.
- 5 Mahajan, A. S., Shaw, M., Oetjen, H., Hornsby, K. E., Carpenter, L. J., Kaleschke, L., Tian-
6 Kunze, X., Lee, J. D., Moller, S. J., Edwards, P., Commane, R., Ingham, T., Heard, D. E., and
7 Plane, J. M. C.: Evidence of reactive iodine chemistry in the Arctic boundary layer, *J. Geophys.*
8 *Res.*, [Atmos.], 115, D20303, doi:10.1029/2009JD013665, 2010b.
- 9 Mahajan, A. S., Gómez Martín, J. C., Hay, T. D., Royer, S. J., Yvon-Lewis, S., Liu, Y., Hu, L.,
10 Prados-Roman, C., Ordóñez, C., Plane, J. M. C., and Saiz-Lopez, A.: Latitudinal distribution of
11 reactive iodine in the Eastern Pacific and its link to open ocean sources, *Atmos. Chem. Phys.*, 12,
12 11609-11617, 10.5194/acp-12-11609-2012, 2012.
- 13 McFiggans, G., Coe, H., Burgess, R., Allan, J., Cubison, M., Alfarra, M. R., Saunders, R., Saiz-
14 Lopez, A., Plane, J. M. C., Wevill, D. J., Carpenter, L. J., Rickard, A. R., and Monks, P. S.:
15 Direct evidence for coastal iodine particles from *Laminaria* macroalgae - linkage to emissions of
16 molecular iodine, *Atmos. Chem. Phys.*, 4, 701-713, 2004.
- 17 Nakano, Y., Ukeguchi, H., and Ishiwata, T.: Rate constant of the reaction of NO₃ with CH₂I₂
18 measured with use of cavity ring-down spectroscopy, *Chem. Phys. Lett.*, 430, 235-239, doi:
19 10.1016/j.cplett.2006.09.002, 2006.



- 1 O'Dowd, C. D., Jimenez, J. L., Bahreini, R., Flagan, R. C., Seinfeld, J. H., Hameri, K., Pirjola,
2 L., Kulmala, M., Jennings, S. G., and Hoffmann, T.: Marine aerosol formation from biogenic
3 iodine emissions, *Nature*, 417, 632-636, 2002.
- 4 Ordóñez, C., Lamarque, J. F., Tilmes, S., Kinnison, D. E., Atlas, E. L., Blake, D. R., Sousa
5 Santos, G., Brasseur, G., and Saiz-Lopez, A.: Bromine and iodine chemistry in a global
6 chemistry-climate model: description and evaluation of very short-lived oceanic sources, *Atmos.*
7 *Chem. Phys.*, 12, 1423-1447, 10.5194/acp-12-1423-2012, 2012.
- 8 Pechtl, S., Lovejoy, E. R., Burkholder, J. B., and von Glasow, R.: Modeling the possible role of
9 iodine oxides in atmospheric new particle formation, *Atmos. Chem. Phys.*, 6, 505-523, 2006.
- 10 Plane, J. M. C., Joseph, D. M., Allan, B. J., Ashworth, S. H., and Francisco, J. S.: An
11 Experimental and Theoretical Study of the Reactions $\text{OIO} + \text{NO}$ and $\text{OIO} + \text{OH}$, *J. Phys. Chem.*
12 *A*, 110, 93-100, 2006.
- 13 Prados-Roman, C., Cuevas, C. A., Fernandez, R. P., Kinnison, D. E., Lamarque, J. F., and Saiz-
14 Lopez, A.: A negative feedback between anthropogenic ozone pollution and enhanced ocean
15 emissions of iodine, *Atmos. Chem. Phys.*, 15, 2215-2224, 10.5194/acp-15-2215-2015, 2015a.
- 16 Prados-Roman, C., Cuevas, C. A., Hay, T., Fernandez, R. P., Mahajan, A. S., Royer, S. J., Galí,
17 M., Simó, R., Dachs, J., Großmann, K., Kinnison, D. E., Lamarque, J. F., and Saiz-Lopez, A.:
18 Iodine oxide in the global marine boundary layer, *Atmos. Chem. Phys.*, 15, 583-593,
19 10.5194/acp-15-583-2015, 2015b.



- 1 Read, K. A., Mahajan, A. S., Carpenter, L. J., Evans, M. J., Faria, B. V. E., Heard, D. E.,
2 Hopkins, J. R., Lee, J. D., Moller, S. J., Lewis, A. C., Mendes, L., McQuaid, J. B., Oetjen, H.,
3 Saiz-Lopez, A., Pilling, M. J., and Plane, J. M. C.: Extensive halogen-mediated ozone
4 destruction over the tropical Atlantic Ocean, *Nature*, 453, 1232-1235, 2008.
- 5 Read, K. A., Lee, J. D., Lewis, A. C., Moller, S. J., Mendes, L., and Carpenter, L. J.: Intra-annual
6 cycles of NMVOC in the tropical marine boundary layer and their use for interpreting seasonal
7 variability in CO, *Journal of Geophysical Research: Atmospheres*, 114, n/a-n/a,
8 10.1029/2009jd011879, 2009.
- 9 Roberston, S. H., Glowacki, D. R., Liang, C. H., Morley, C., Shannon, R., Blitz, M., and Pilling,
10 M. J.: MESMER (Master Equation Solver for Multi-Energy Well Reactions), 2008–2012: An
11 object oriented C++ program for carrying out ME calculations and eigenvalue-eigenvector
12 analysis on arbitrary multiple well systems, edited. [Available at
13 <http://sourceforge.net/projects/mesmer/>], in, 4.1 ed., 2014.
- 14 Roscoe, H. K., Jones, A. E., Brough, N., Weller, R., Saiz-Lopez, A., Mahajan, A. S.,
15 Schoenhardt, A., Burrows, J. P., and Fleming, Z. L.: Particles and iodine compounds in coastal
16 Antarctica, *Journal of Geophysical Research: Atmospheres*, 120, 7144-7156,
17 10.1002/2015jd023301, 2015.
- 18 Saiz-Lopez, A., and Plane, J. M. C.: Novel iodine chemistry in the marine boundary layer,
19 *Geophys. Res. Lett.*, 31, L04112, 2004.



- 1 Saiz-Lopez, A., Plane, J. M. C., McFiggans, G., Williams, P. I., Ball, S. M., Bitter, M., Jones, R.
2 L., Hongwei, C., and Hoffmann, T.: Modelling molecular iodine emissions in a coastal marine
3 environment: the link to new particle formation, *Atmos. Chem. Phys.*, 6, 883-895, 2006.
- 4 Saiz-Lopez, A., Plane, J. M. C., Mahajan, A. S., Anderson, P. S., Bauguitte, S. J.-B., Jones, A.
5 E., Roscoe, H. K., Salmon, R. A., Bloss, W. J., Lee, J. D., and Heard, D. E.: On the vertical
6 distribution of boundary layer halogens over coastal Antarctica: implications for O₃, HO_x, NO_x
7 and the Hg lifetime, *Atmos. Chem. Phys.*, 8, 887-900, 2008.
- 8 Saiz-Lopez, A., Lamarque, J.-F., Kinnison, D., Tilmes, S., Ordóñez, C., Orlando, J. J., Conley,
9 A. J., Plane, J. M. C., Mahajan, A., Sousa Santos, G., Atlas, E., Blake, D. R., Sander, S. P.,
10 Schauffler, S. M., Thompson, A. M., and Brasseur, G.: Estimating the climate significance of
11 halogen-driven ozone loss in the tropical marine troposphere, *Atmos. Chem. Phys.*, 12, 3939-
12 3949, 2012a.
- 13 Saiz-Lopez, A., Plane, J. M. C., Baker, A. R., Carpenter, L. J., Von Glasow, R., Gómez Martín,
14 J. C., McFiggans, G., and Saunders, R. W.: Atmospheric Chemistry of Iodine, *Chem. Rev.*
15 (Washington, DC, U. S.), 112, 1773-1804, 10.1021/cr200029u, 2012b.
- 16 Saiz-Lopez, A., Fernandez, R. P., Ordóñez, C., Kinnison, D. E., Gómez Martín, J. C., Lamarque,
17 J. F., and Tilmes, S.: Iodine chemistry in the troposphere and its effect on ozone, *Atmos. Chem.*
18 *Phys.*, 14, 13119-13143, 10.5194/acp-14-13119-2014, 2014.
- 19 Saiz-Lopez, A., Baidar, S., Cuevas, C. A., Koenig, T. K., Fernandez, R. P., Dix, B., Kinnison, D.
20 E., Lamarque, J. F., Rodriguez-Lloveras, X., Campos, T. L., and Volkamer, R.: Injection of
21 iodine to the stratosphere, *Geophys. Res. Lett.*, n/a-n/a, 10.1002/2015gl064796, 2015.



- 1 Sander, S. P., Orkin, V. L., Kurylo, M. J., Golden, D. M., Huie, R. E., Kolb, C. E., Finlayson-
2 Pitts, B. J., Molina, M. J., Friedl, R. R., Ravishankara, A. R., Moortgat, G. K., Keller-Rudek, H.,
3 and Wine, P. H.: Chemical kinetics and photochemical data for use in atmospheric studies, JPL-
4 NASA, 2006.
- 5 Saunders, R. W., and Plane, J. M. C.: Formation Pathways and Composition of Iodine Oxide
6 Ultra-Fine Particles, *Environ. Chem.*, 2, 299-303, 2005.
- 7 Sherwen, T., Evans, M. J., Carpenter, L. J., Andrews, S. J., Lidster, R. T., Dix, B., Koenig, T. K.,
8 Sinreich, R., Ortega, I., Volkamer, R., Saiz-Lopez, A., Prados-Roman, C., Mahajan, A. S., and
9 Ordóñez, C.: Iodine's impact on tropospheric oxidants: a global model study in GEOS-Chem,
10 *Atmos. Chem. Phys.*, 16, 1161-1186, 10.5194/acp-16-1161-2016, 2016.
- 11 Simpson, W. R., Brown, S. S., Saiz-Lopez, A., Thornton, J. A., and Glasow, R. v.: Tropospheric
12 Halogen Chemistry: Sources, Cycling, and Impacts, *Chem. Rev.*, 115, 4035-4062,
13 10.1021/cr5006638, 2015.
- 14 Sommariva, R., Bloss, W. J., and von Glasow, R.: Uncertainties in gas-phase atmospheric iodine
15 chemistry, *Atmos. Environ.*, 57, 219-232, doi: 10.1016/j.atmosenv.2012.04.032, 2012.
- 16 Volkamer, R., Baidar, S., Campos, T. L., Coburn, S., DiGangi, J. P., Dix, B., Eloranta, E. W.,
17 Koenig, T. K., Morley, B., Ortega, I., Pierce, B. R., Reeves, M., Sinreich, R., Wang, S., Zondlo,
18 M. A., and Romashkin, P. A.: Aircraft measurements of BrO, IO, glyoxal, NO₂, H₂O, O₂-O₂
19 and aerosol extinction profiles in the tropics: comparison with aircraft-/ship-based in situ and
20 lidar measurements, *Atmos. Meas. Tech.*, 8, 2121-2148, 10.5194/amt-8-2121-2015, 2015.



1 von Glasow, R., Sander, R., Bott, A., and Crutzen, P. J.: Modeling halogen chemistry in the
2 marine boundary layer. 1. Cloud-free MBL, *J. Geophys. Res.*, 107, 4341, 2002.

3 Wachsmuth, M., Gäggeler, H. W., von Glasow, R., and Ammann, M.: Accommodation
4 coefficient of HOBr on deliquescent sodium bromide aerosol particles, *Atmos. Chem. Phys.*, 2,
5 121-131, 10.5194/acp-2-121-2002, 2002.

6 Wang, F., Saiz-Lopez, A., Mahajan, A. S., Gómez Martín, J. C., Armstrong, D., Lemes, M., Hay,
7 T., and Prados-Roman, C.: Enhanced production of oxidised mercury over the tropical Pacific
8 Ocean: a key missing oxidation pathway, *Atmos. Chem. Phys.*, 14, 1323-1335, 10.5194/acp-14-
9 1323-2014, 2014.

10

11

12

1 **Tables**

2

 3 Table 1: Night time reactions of emitted inorganic iodine compounds considered in addition to
 4 the iodine chemistry scheme used by (Saiz-Lopez et al., 2014).

No.	Reaction	Notes
R1.	$I_2 + NO_3 \rightarrow I + IONO_2$	$1.5 \times 10^{-12} \text{ cm}^3 \text{ molecule}^{-1} \text{ s}^{-1}$ [Chambers et al., 1992]
R2.	$HOI + NO_2 \rightarrow I + HNO_3$	Endothermic by 9 kJ mol^{-1} and the transition state is 73 kJ mol^{-1} above the reactants
R3.	$HOI + HNO_3 \rightarrow IONO_2 + H_2O$	Exothermic by 11 kJ mol^{-1} . The reaction first forms a complex 21 kJ mol^{-1} below the reactants but this rearranges to the products via a transition state that is 110 kJ mol^{-1} above the reactants.
R4.	$HOI + NO_3 \rightarrow IO + HNO_3$	Exothermic by 11 kJ mol^{-1} with all transition states below the reactants. $k(T) = 2.7 \times 10^{-12} (300 \text{ K} / T)^{2.66} \text{ cm}^3 \text{ molecule}^{-1} \text{ s}^{-1}$

5

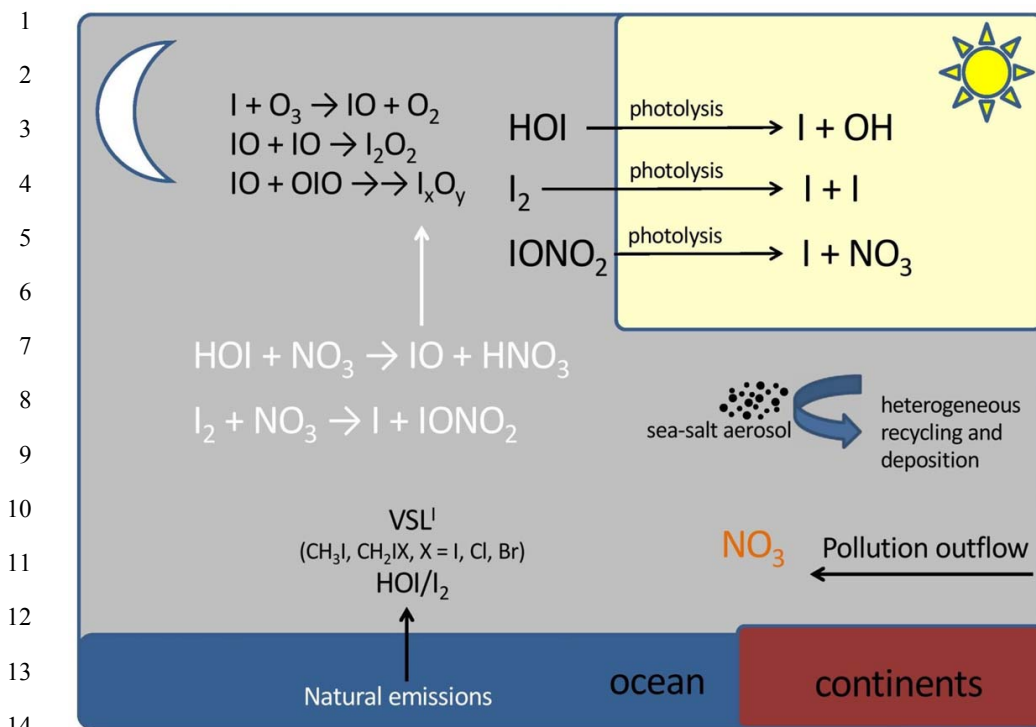
6



1 **Table 2.** Calculated vibrational frequencies, rotational constants and energies of the stationary
 2 points and asymptotes on the HOI + NO₃ doublet potential energy surface

Species	Geometry ^a	Vibrational frequencies ^b	Rotational constants ^c	Potential energy ^d
HOI + NO ₃		603, 1084, 3803 & 261, 261, 805, 1108, 1108, 1126	623.9, 8.182, 8.076 & 13.84, 13.84, 6.919	0.0
IOH-NO ₃ complex	O 1.623, 0.284, -0.331 H 1.484, -0.657, -0.043 I 0.009, 1.205, 0.286 N -0.456, -2.265, 0.030 O -1.052, -3.321, -0.0473 O -1.147, -1.195, -0.228 O 0.742, -2.161, 0.333	55, 84, 118, 161, 196, 615, 629, 667, 705, 803, 968, 1228, 1273, 1491, 3268	5.610, 0.916, 0.806	-24.0
IO-H-NO ₂ TS	O 0.309, 1.515, 0.247 H -0.834, 1.314, -0.017 I 1.280, -0.089, -0.093 N -2.349, -0.133, 0.019 O -3.518, -0.429, -0.035 O -1.444, -0.962, 0.257 O -2.019, 1.117, -0.187	1249i, 70, 97, 103, 225, 472, 676, 698, 797, 806, 1041, 1147, 1308, 1513, 1626	6.300, 0.864, 0.767	-16.4
IO-HNO ₃ complex	O 0.571, 1.350, 0.348 H -1.111, 1.098, -0.020 I 1.870, 0.0645, -0.152 N -2.503, -0.202, 0.0186 O -3.673, -0.396, -0.170 O -1.654, -0.986, 0.401 O -2.081, 1.090, -0.242	35, 43, 76, 126, 198, 623, 677, 703, 772, 798, 939, 1331, 1416, 1713, 3281	7.058, 0.605, 0.566	-34.8
IO + HNO ₃		648 & 477, 585, 649, 782, 901, 1320, 1345, 1738, 3724	9.844 & 13.01, 12.05, 6.258	-10.6

3 ^a Cartesian co-ordinates in Å. ^b In cm⁻¹. ^c In GHz. ^d In kJ mol⁻¹, including zero-point energy and spin-orbit coupling of I and IO (see text).
 4

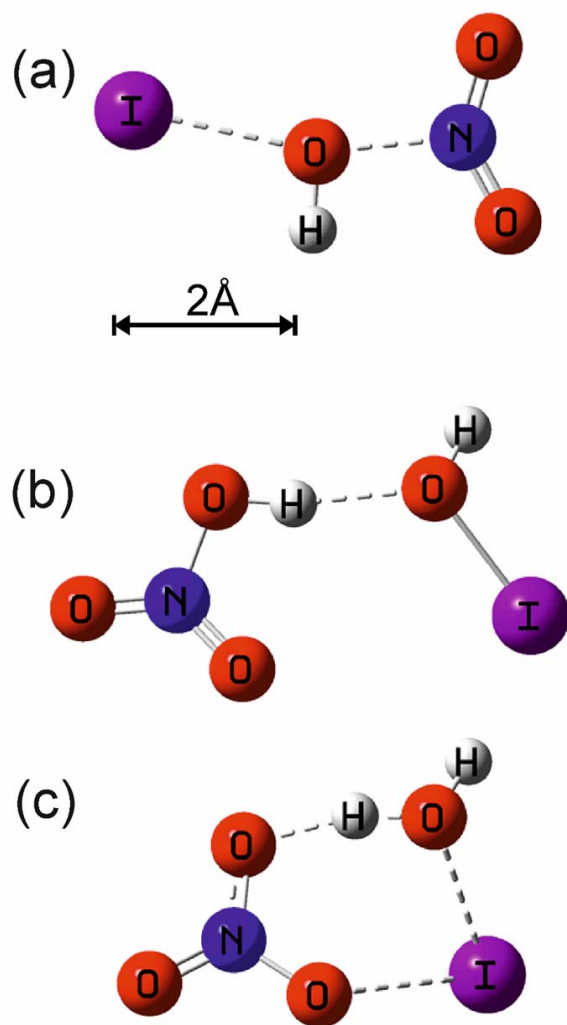


15 **Figure 1.** New nocturnal iodine chemistry (in white) implemented in the THAMO and CAM-
 16 Chem models.

17
 18
 19
 20
 21
 22
 23
 24
 25



1



2

3

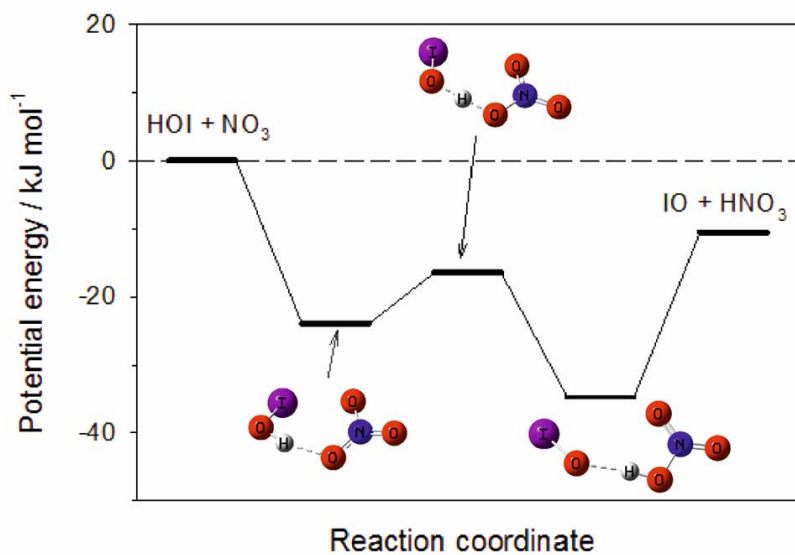
4

5 **Figure 2:** (a) Transition state for the reaction between HOI and NO₂ to form HNO₃ + I; (b)
6 complex formed between HOI and HNO₃, which then reacts via transition state (c) to form
7 IONO₂ + H₂O.

30



1

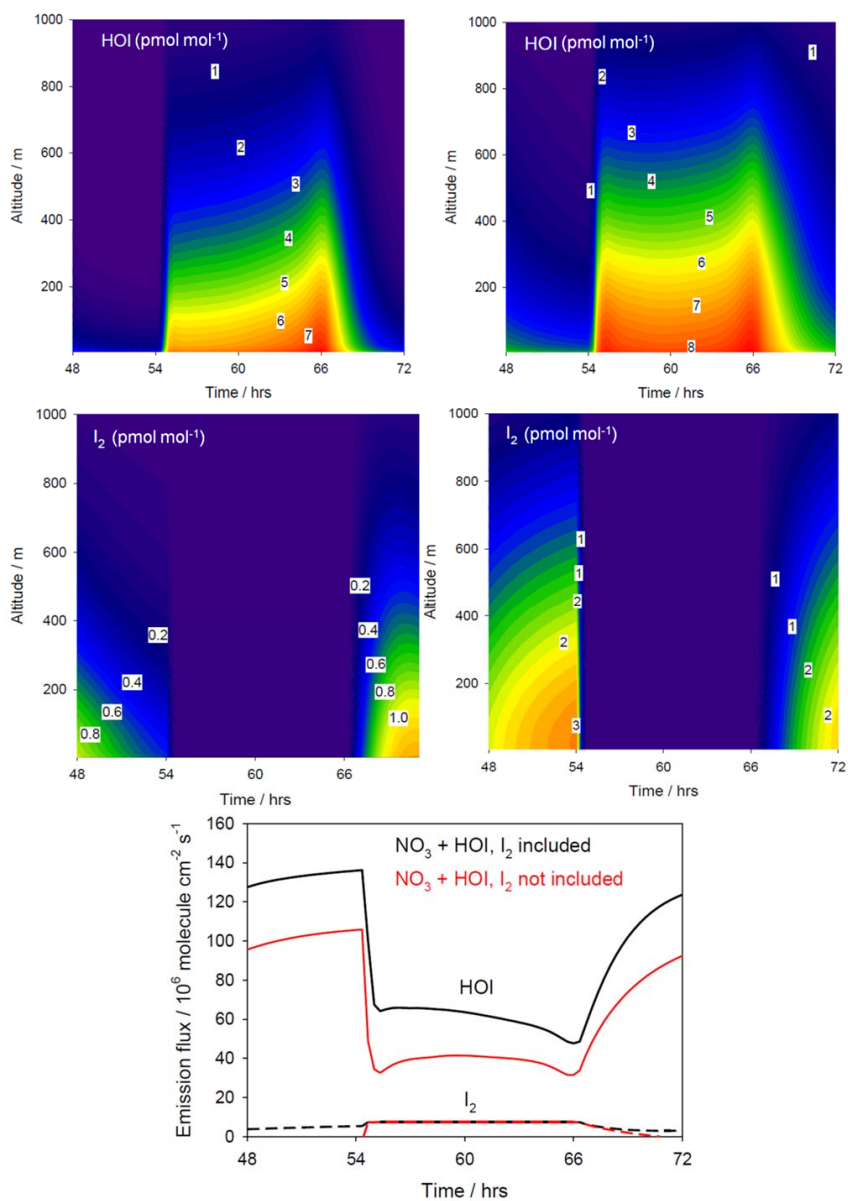


2

3

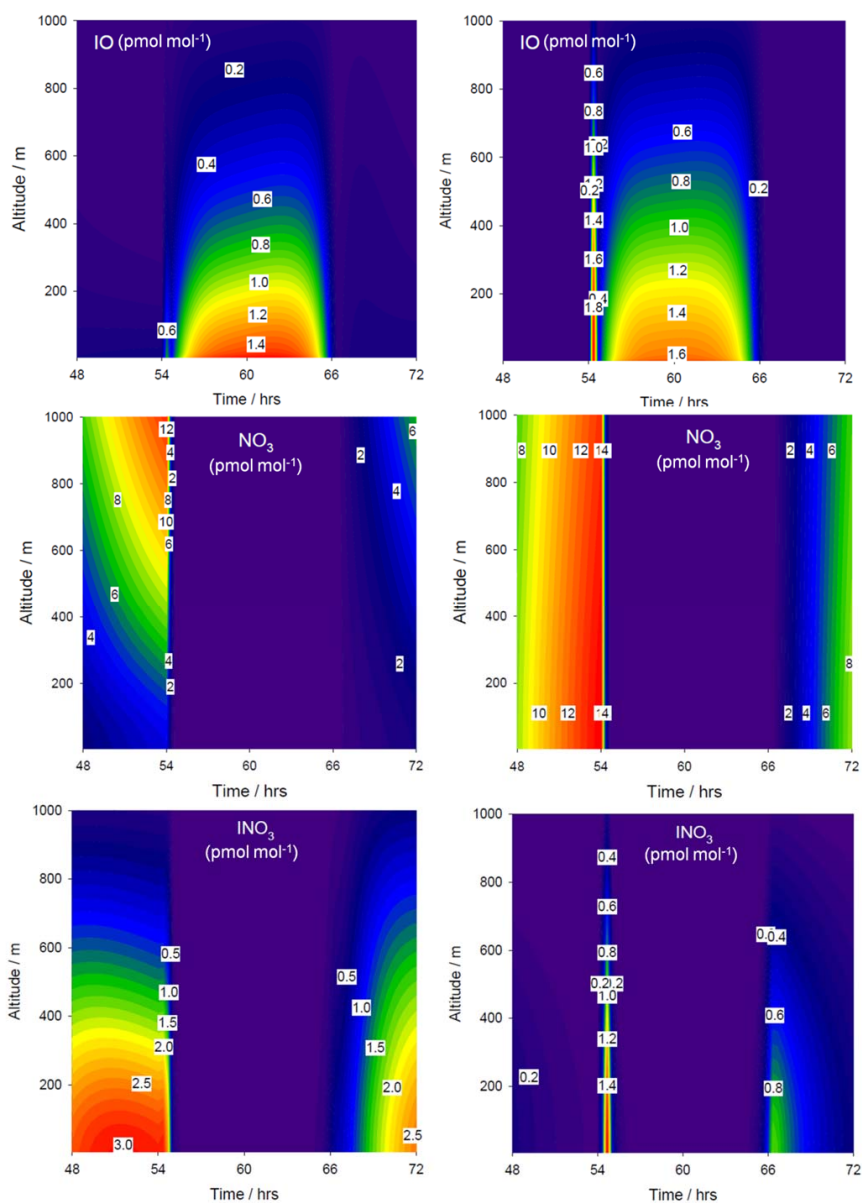
4 **Figure 3.** Potential energy surface for the reaction between HOI and NO₃, which contains two
5 intermediate complexes separated by a submerged barrier.

6



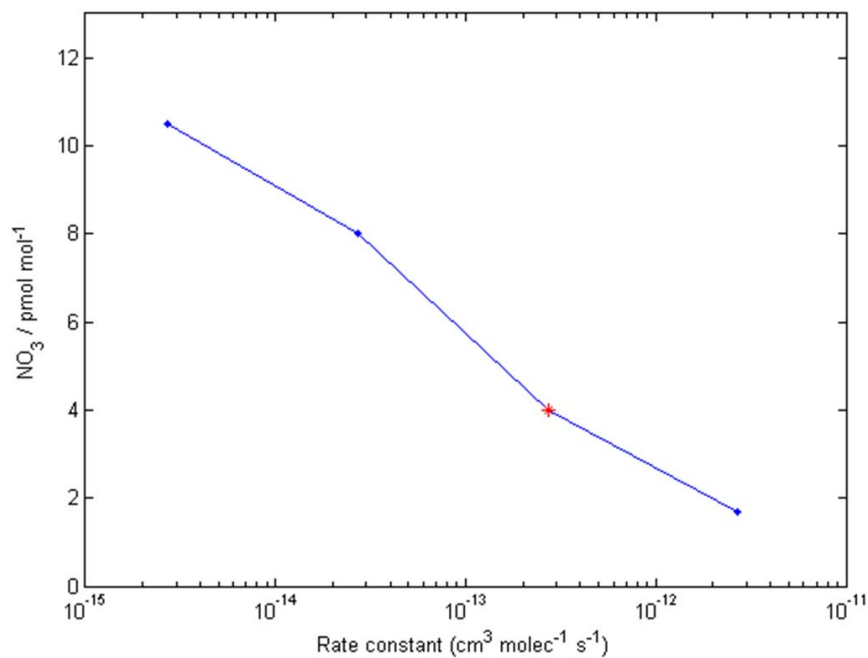
1

2 **Figure 4.** THAMO modeled diurnal variation of HOI, I₂ and the HOI/I₂ flux from the ocean
3 surface. The right hand panels are from scenario 1, which do not include night time reactions of
4 HOI and I₂ with NO₃, while the left hand panels include the reactions in scenario 2.



1

2 **Figure 5.** THAMO modeled diurnal variation of IO, NO₃ and the IONO₂. The right hand panels
3 are from scenario 1, which do not include night time reactions of HOI and I₂ with NO₃, while the
4 left hand panels include the reactions in scenario 2.



1

2 **Figure 6.** Sensitivity run showing the effect of the uncertainty in the rate constant estimation on
3 the reduction of NO_3 at the surface - the red point is the theoretical estimate.

4

5

6

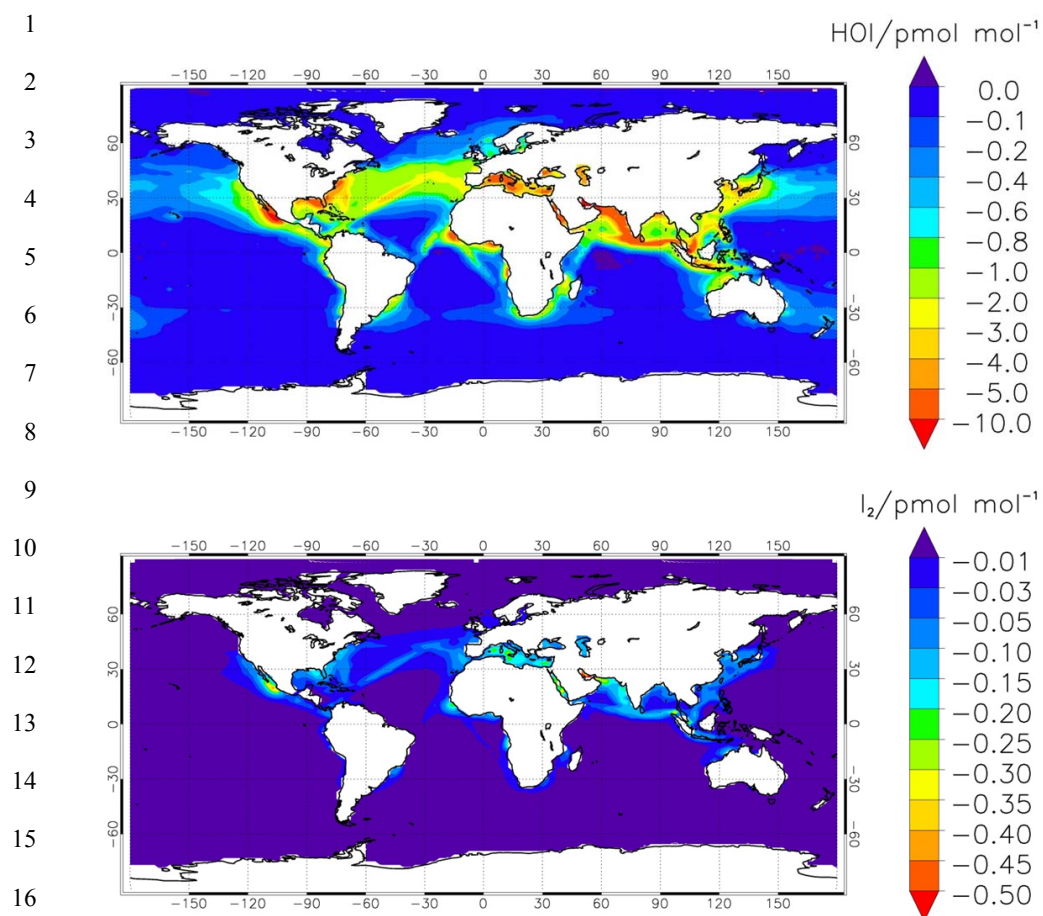
7

8

9

10

11



18 **Figure 7.** Modelled annual average of HOI (a) and I_2 (b) during night. The panels show the
19 difference in vertical mixing ratio between the simulations with and without reactions (1) and
20 (2).

21

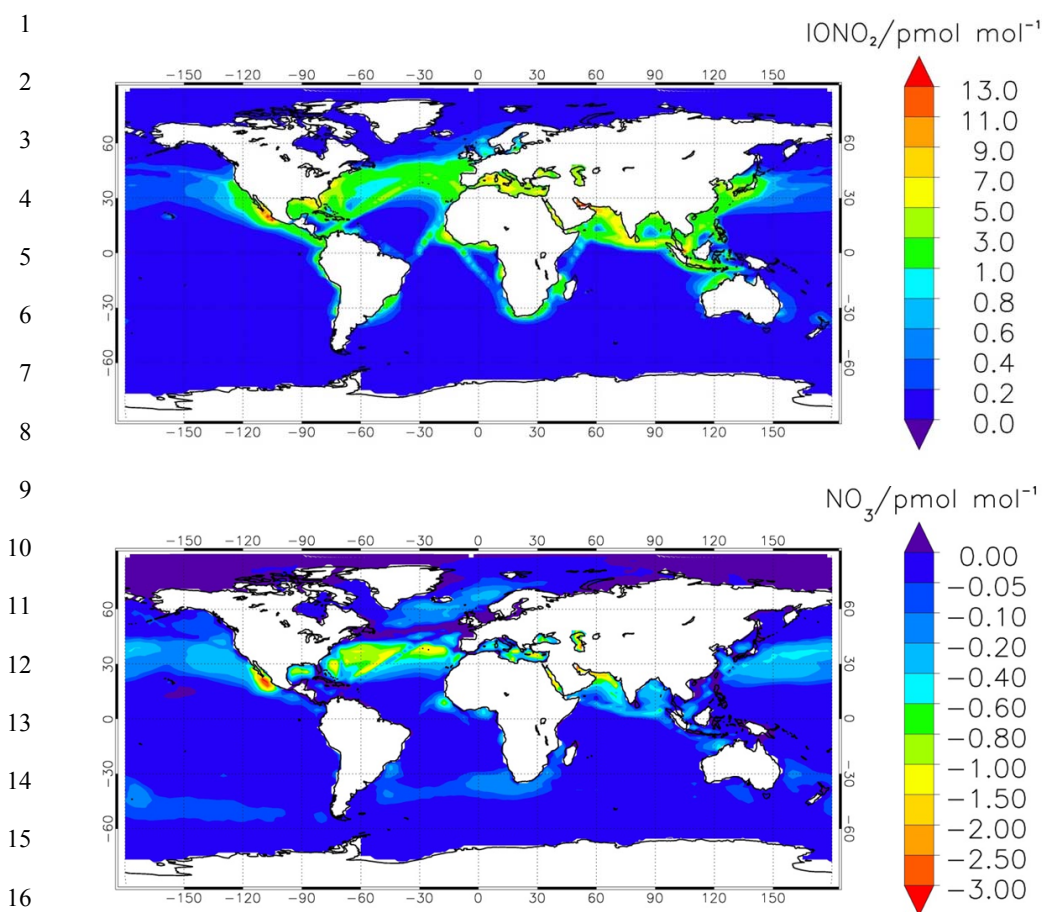
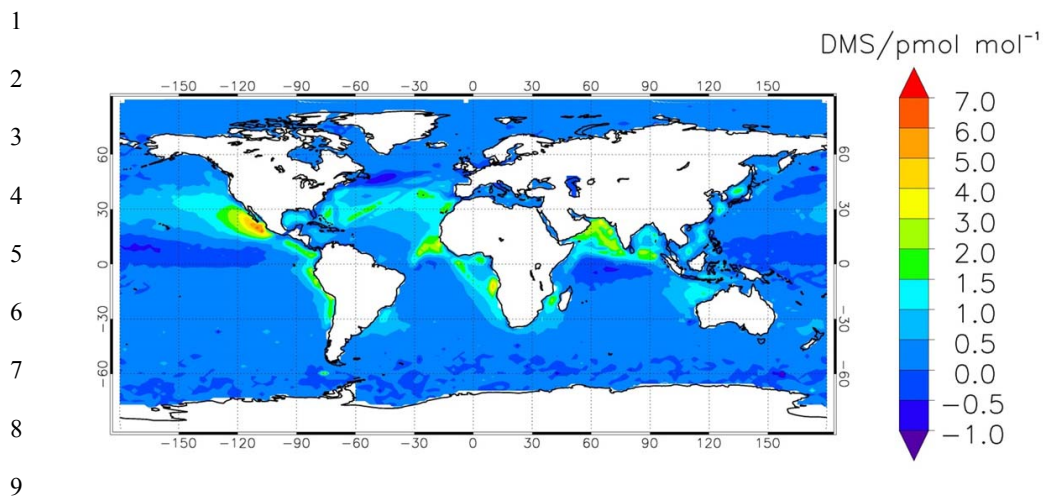
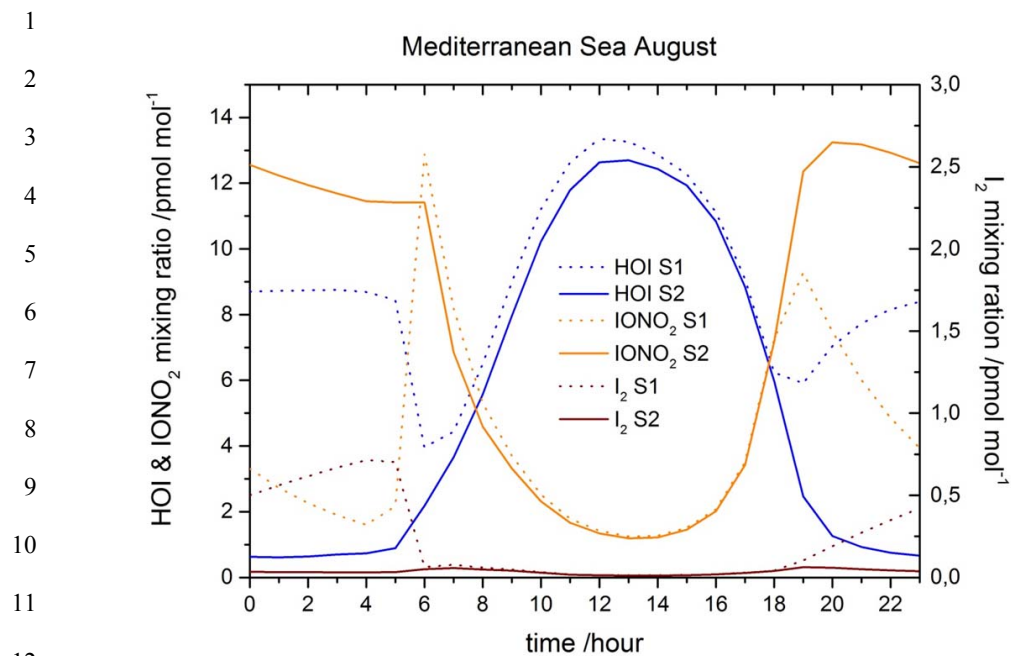


Figure 8. Modelled annual average of IONO₂ (a) and NO₃ (b) during night time over the ocean surface, as the difference in volume mixing ratio between the simulations with and without reactions (1) and (2).



10 **Figure 9.** Increase in the DMS levels at night time over the ocean surface due to the inclusion of
11 the reactions R1 and R2 in CAM-Chem.

12
13
14
15
16
17
18
19
20
21
22
23
24

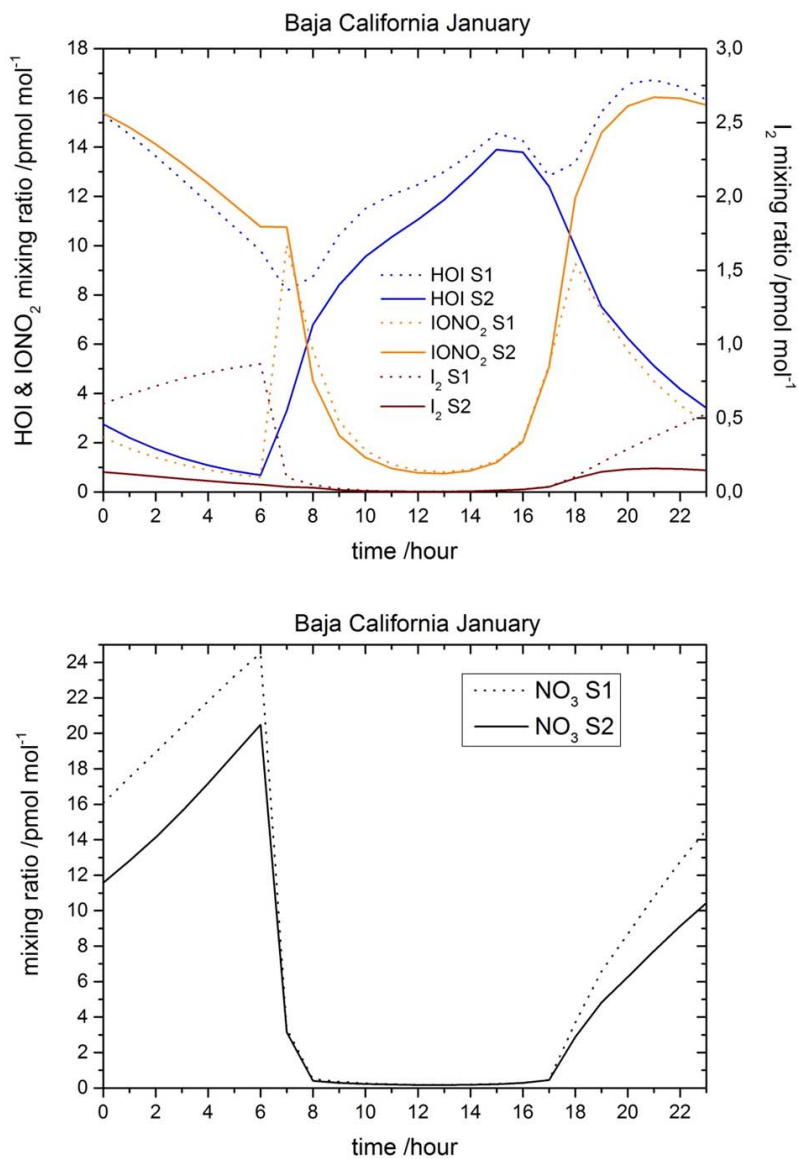


13 **Figure 10.** Hourly averaged concentration of HOI, IONO₂ and I₂ in the Mediterranean Sea at
14 surface level (lon:10°→20°E, lat:33°→40°N)

15
16
17
18
19
20
21
22
23
24



1
2
3
4
5
6
7
8
9
10
11
12
13
14
15
16
17
18
19
20
21



22 **Figure 11.** Hourly averaged concentration of HOI, IONO₂ and I₂ (upper panel) and NO₃ (bottom
23 panel) in the Pacific Ocean close to Baja California (lon:-110°→-106°E, lat:16°→23°N)